



This is a repository copy of *Strong coupling of organic dyes located at the surface of a dielectric slab microcavity*.

White Rose Research Online URL for this paper:
<https://eprints.whiterose.ac.uk/185388/>

Version: Accepted Version

Article:

Georgiou, K., Jayaprakash, R. orcid.org/0000-0002-2021-1601 and Lidzey, D.G. orcid.org/0000-0002-8558-1160 (2020) Strong coupling of organic dyes located at the surface of a dielectric slab microcavity. *The Journal of Physical Chemistry Letters*, 11 (22). pp. 9893-9900. ISSN 1948-7185

<https://doi.org/10.1021/acs.jpcclett.0c02751>

This document is the Accepted Manuscript version of a Published Work that appeared in final form in *Journal of Physical Chemistry Letters*, copyright © American Chemical Society after peer review and technical editing by the publisher. To access the final edited and published work see <https://doi.org/10.1021/acs.jpcclett.0c02751>.

Reuse

Items deposited in White Rose Research Online are protected by copyright, with all rights reserved unless indicated otherwise. They may be downloaded and/or printed for private study, or other acts as permitted by national copyright laws. The publisher or other rights holders may allow further reproduction and re-use of the full text version. This is indicated by the licence information on the White Rose Research Online record for the item.

Takedown

If you consider content in White Rose Research Online to be in breach of UK law, please notify us by emailing eprints@whiterose.ac.uk including the URL of the record and the reason for the withdrawal request.



eprints@whiterose.ac.uk
<https://eprints.whiterose.ac.uk/>

Strong Coupling of Organic Dyes Located at the Surface of a Dielectric Slab

Microcavity

K. Georgiou^{1,*}, R. Jayaprakash and D.G. Lidzey*

Department of Physics and Astronomy, University of Sheffield, Hicks Building, Hounsfield Road, Sheffield S3 7RH, United Kingdom

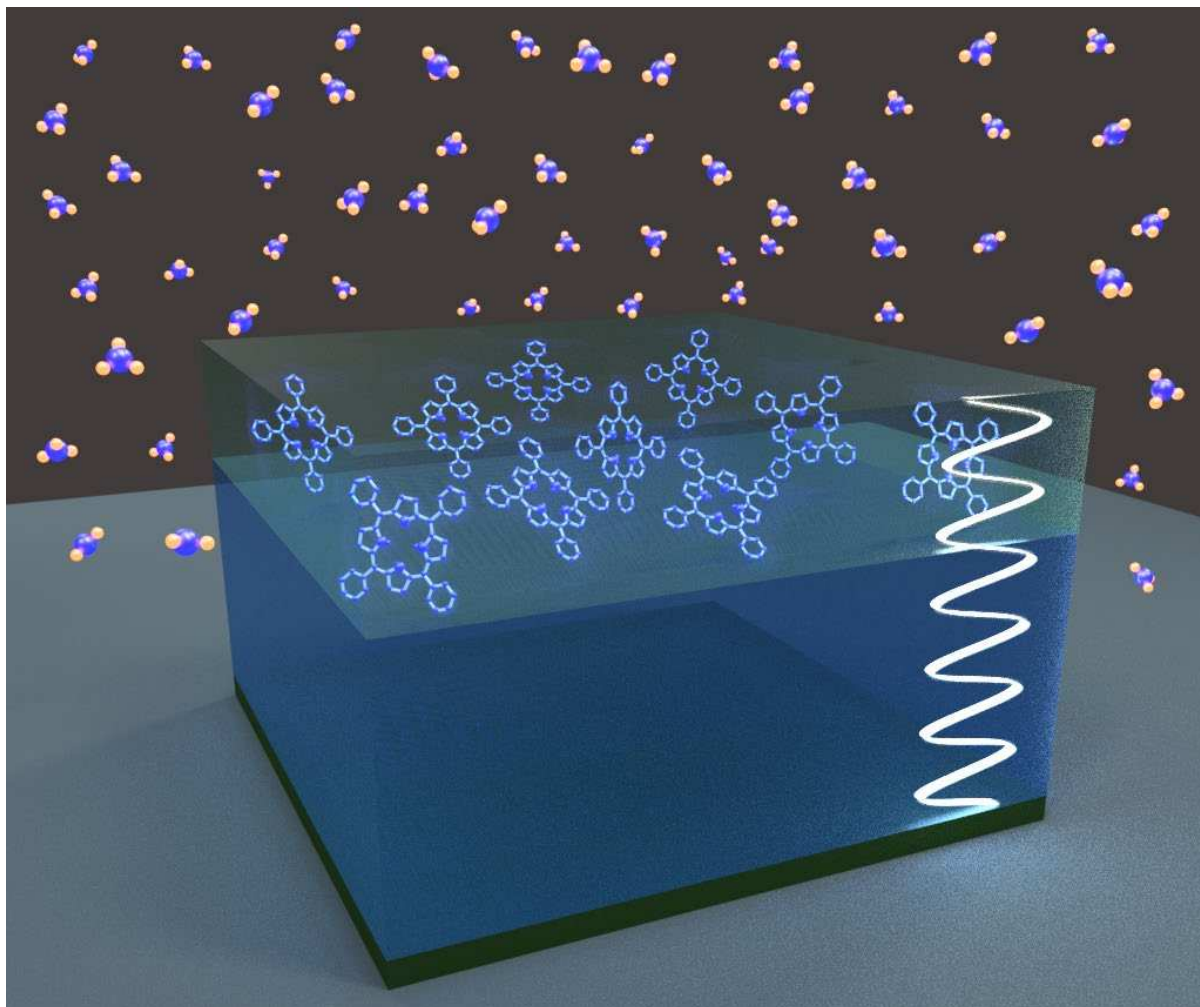
* email: k.georgiou@sheffield.ac.uk , d.g.lidzey@sheffield.ac.uk

ABSTRACT

Strong coupling to the electronic or vibronic transitions of an organic semiconductor has been extensively studied in microcavity structures in which a molecular film is placed between two closely spaced mirrors. Recent experiments suggest that such strong coupling can be used to modify chemical reactions, however the geometry of conventional microcavity structures makes such studies difficult as they limit the ability of molecules to interact with their local environment. Here, we show that optical strong coupling to a molecular film can be achieved even when such molecules are located on the surface of a dielectric slab. We then show that such molecules on the surface of the slab can undergo facile interactions with molecules in their surrounding environment, and evidence a reversible protonation / deprotonation reaction by exposing a surface-bound porphyrin to an acidic or basic vapour. Although our proof-of-principle measurements do not evidence any change in reaction rates, we believe our structures represent a promising system in which to explore polariton-driven chemical phenomena.

¹ Current Address: Department of Physics, University of Cyprus, P. O. Box 20537, Nicosia 1678, Cyprus

Table of Contents Graphic



Keywords: Organic Polariton, Polariton Chemistry, Dielectric Slab, Polariton Sensor, Open Resonator

INTRODUCTION

Microcavity exciton-polaritons are bosonic quasiparticles resulting from the strong coupling of a confined photonic field to semiconductor excitons¹. Frenkel-like excitons in organic semiconductors have attracted particular attention for microcavity strong coupling due to their large binding energy that confers stability at room temperature²⁻⁷. The most widely explored optical structure that has been used to realise polaritonic states is the Fabry-Perot resonator. Such resonators consist of two planar, highly reflective mirrors positioned in close proximity either side of a semiconducting material. Here, the confined optical modes of the cavity can undergo strong coupling with the semiconductor excitons, resulting in the formation of cavity-polariton states⁸.

Recently, interest has grown in the nascent field of polaritonic chemistry. This emerging discipline is positioned at the crossroads between cavity quantum electrodynamics and chemistry. Here, it has been experimentally demonstrated⁹⁻¹⁶ that it is possible to alter the potential energy surfaces and change chemical reaction rates of a molecule by strong coupling its electronic or vibrational transitions to confined photons in a cavity, stimulating much theoretical research¹⁷⁻²¹. Furthermore by probing photo- or chemically-induced changes of the optical properties of strongly coupled molecules via changes in their polaritonic eigenstates^{22,23}, polaritonic structures can act as a platform for sensing applications. Unfortunately however, the realisation of optical strong coupling and accompanying polaritonic phenomena are most often evidenced in devices in which two high-reflectivity mirrors are deposited either side of a semiconductor layer forming a heterostructure²⁴. This presents a potential problem as the ‘encapsulation’ of molecules by the cavity mirrors limits the ability of the strongly coupled molecules to undergo chemical reactions with other chemical species that might be in a liquid or gaseous form, or might involve a process in which a molecular film softens or swells. This problem can be circumvented through the use of cavities

in which the cavity mirrors are physically separated by several microns, e.g. through the use of piezo-electric stages^{25,26} or other types of spacer layer^{10,14,16}, with liquid then being introduced into the cavity region. However, such microcavity structures can be rather delicate and may not be straightforward to scale-up as part of a practical manufacture process.

An alternate approach is to couple excitonic transitions to surface plasmon resonances, forming plasmon exciton-polaritons. Such resonances are comparatively lossy, with the confined field being localised very close to the surface of the metal⁸. This limits the formation of polaritonic states to molecules that are located in close proximity to the metal surface and thus reduces the number of molecules whose properties can be modified by strong coupling. Furthermore, to optically probe such states, it is necessary to match the in-plane momentum of light to optical states within the light-cone; a process that is usually achieved through periodic patterning of the metallic surface to create localised plasmonic modes. This patterning process can make the design and fabrication of such structures complicated and demanding²⁷⁻²⁹. Although ‘sensor’ activity has been demonstrated in plasmonic nanostructures³⁰, a further drawback is the possibility of chemical reactions between metals and organic molecules at their surface, or solvents and gaseous analytes in the vicinity of the metallic surface. For this reason, metallic nanostructures are non-ideal systems in which to explore polaritonic chemistry.

We note that other all-dielectric ‘open’ structures have also been used to explore strong coupling. For example, recent work has shown that metasurfaces can be used to demonstrate strong coupling between organic molecules and Mie surface lattice resonances^{31,32}. High Q-factor microcavities have also been used to couple excitonic transitions to evanescent fields of slab or Bloch surface waves^{33,34}. However, such structures generally require the use of precise fabrication techniques that increase their cost and complexity, or need imaging setups to match the in-plane momentum of light with the optical states within the light-cone.

In this paper, we propose and realise organic exciton-polaritons at room temperature using a simple dielectric slab resonator that allows direct physical access to the strongly coupled molecular species. This structural geometry circumvents previous limitations imposed within ‘encapsulated’ Fabry-Perot heterostructures and allows such molecules to directly interact with their local chemical environment. We evidence this chemical interaction whilst the molecules are strong-coupled by following a simple protonation / deprotonation by exposing the molecular species at the surface to an acidic / basic vapour. We then show that strong-coupling effect can still be evidenced while such structures are fully immersed in water. We emphasize that our measurements *do not explore chemical reaction rates*, and thus *we do not determine* whether polaritonic effects in our structures can be used to modify chemical reactions. Nevertheless, we believe that our proof-of-principle measurements demonstrate that such structures may form an effective basis for further polariton-chemistry studies.

RESULTS AND DISCUSSION

Figure 1a shows a schematic of the resonators used in this study. To fabricate such structures, a Nb₂O₅ film was evaporated on to a quartz-coated glass substrate followed by a thick SiO₂ layer. Finally an organic semiconductor film was deposited onto the SiO₂ by spin casting. Figure 1a shows the distribution of the electric field within the various layers of the structure calculated using a transfer matrix reflectivity (TMR) model assuming that the organic semiconductor layer has a refractive index of 1.69. The electric field distribution near exciton-photon resonance is also shown in more detail in Figure 1b, where simulations are shown for two different dielectric slab resonators that consist of different thicknesses of Nb₂O₅, SiO₂, with the organic-semiconductor layer again assumed to have a refractive index of $n = 1.69$. Here, we identify the various layers in the multilayer stack using colour shading as a guide to the eye, with refractive index values for the Nb₂O₅, SiO₂ and organic-semiconductor layers assumed as 2.15, 1.46 and 1.69 respectively.

The confined electrical field evident in Figure 1b results from reflection by the refractive index changes between the SiO_2 and Nb_2O_5 and between the organic film and the surrounding air, with reflectivity coefficients at normal incidence of 4% and 7% respectively calculated using Fresnel equations.³⁵ This results in the formation of optical cavities having a Q-factor of 13 and 33 for the thinner and thicker dielectric slabs respectively. In both cases, the cavity finesse is ~ 2 (defined as the ratio of the cavity free spectral range to cavity mode linewidth)⁸. As we show below the amplitude of the optical field within the organic layer is sufficiently large to allow strong light-matter interactions to take place despite the relatively low reflectivity and finesse of such structures.

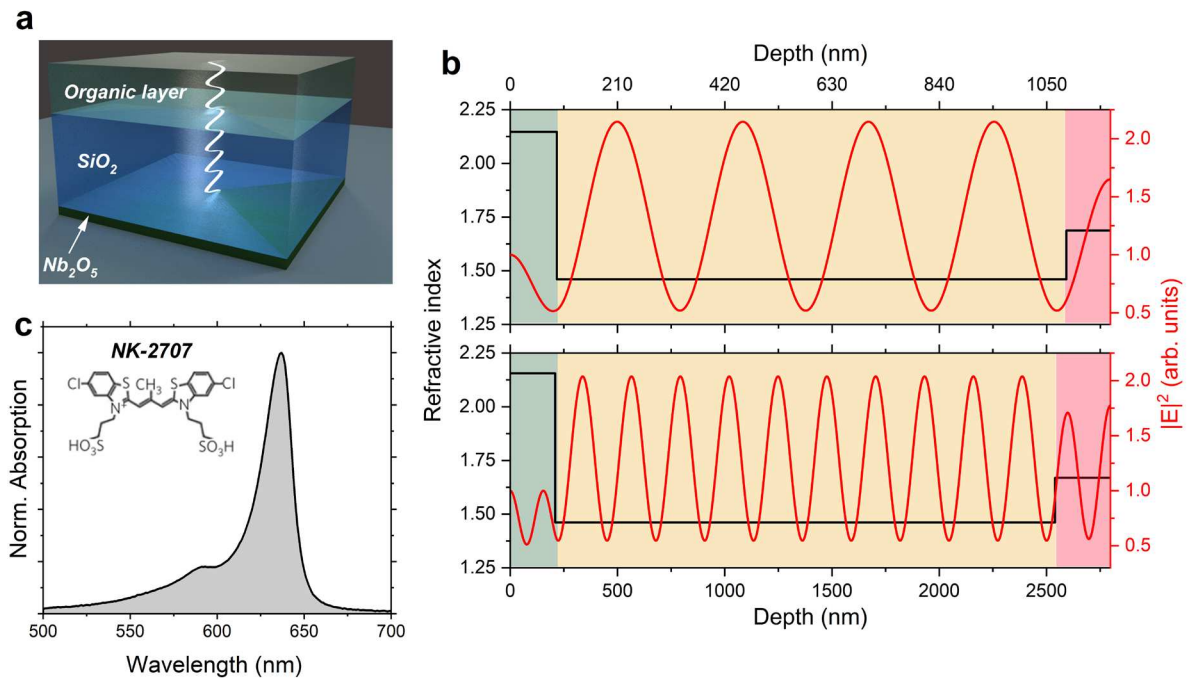


Figure 1. Dielectric slab microcavities coated with organic semiconductors. (a) Schematic of a dielectric slab microcavity coated with an organic semiconductor of refractive index of 1.69 along with the distribution of the electric field in the various layers calculated using a TMR model. (b) Electric field distribution along the various layers of two structures composed of Nb_2O_5 / SiO_2 / Organic-semiconductor layers respectively, with the layers having the following thicknesses: (top) 100 / 1000 / 100 nm and (bottom) 200 / 2300 / 250 nm. These layers are defined in the model

through their refractive index. Additionally, a different colour shading for each layer (Nb₂O₅ - green, SiO₂ - yellow and Organic-semiconductor - red) is used in the background of the plot as a guide to the eye. (c) Normalised absorption spectrum of a 180 nm thin film of NK-2707 / gelatine blend. The chemical structure of NK-2707 is shown in the inset.

We have placed a series of different organic semiconductors on top of this structure. The first material we discuss is the cyanine dye 5-chloro-2-[3-[5-chloro-3-(3-sulphopropyl)-2(3H)-benzothiazolylidene]-2-methyl-1-propenyl]-3-(3-sulphopropyl) benzothiazolium hydroxide, inner salt, compound with triethylamine (manufacturer's code NK-2707). When this dye is dissolved in a polar solvent, it undergoes self-organisation and forms a J-aggregate that has a red-shifted and spectrally narrow absorption and emission transitions compared to its monomeric form³⁶. As a result of high oscillator strength and narrow excitonic linewidth at room temperature, such J-aggregated molecular dyes have been used extensively in polaritonic-based structures and devices³⁷⁻⁴⁰. Figure 1c shows an absorption spectrum of a 180 nm thick film of NK-2707 / gelatine blend deposited on a quartz-coated glass substrate by spin-coating, with the molecular structure of the NK-2707 dye shown in the inset. As it can be seen, the film is characterised by a sharp, narrow excitonic transition centred at around 638 nm. Surface profilometry measurements indicate that such gelatine/NK-2707 films were highly uniform in thickness and had a surface roughness of around 1 nm. As a result of the excellent optical properties of such films, they could be used as the top 'reflecting' surface of the dielectric slab microcavities explored here without introducing significant optical scattering.

Figures 2a and b show angle-resolved white light reflectivity measurements (see Experimental Methods in the Supporting Information) of an open resonator prior to the deposition of an organic semiconducting film. Here, a series of standing optical modes are supported within the low-index SiO₂ layer whose energy and distribution can be tuned by adjusting slab thickness. The data shown in Figure 2a corresponds to a structure consisting of

Nb₂O₅ / SiO₂ layers of thickness 100 / 1000 nm, while data shown in Figure 2b corresponds to a resonator having layer thicknesses of 200 / 2300 nm respectively. We overlay the experimental reflectivity data colour-map with a simulation of the photon-mode dispersion calculated using a TMR model (plotted using white lines). Here, our TMR model indicates that the optical modes evident in Figure 2a correspond to 3rd and 4th order confined photonic modes. As expected, we find that the structure composed of thicker dielectric layers is characterised by more closely separated optical modes. Here, five optical modes are observed in the reflectivity map shown in Figure 2b which our model indicates as being 7th, 8th, 9th, 10th and 11th order modes. For completeness, we plot cross sections of the reflectivity contours recorded at individual angles in Figure S1a and b of the Supporting Information.

We have measured angle-resolved white light reflectivity from the two different thickness slab resonators when coated with a film of NK-2707. In Figure 2c we plot the reflectivity spectrum of the structure shown in Figure 2a. Here it can be seen that the 4th order optical mode becomes resonant with the organic exciton (whose peak absorption wavelength is marked with a white dashed horizontal line) at an angle of $\sim 35^\circ$. At this point, an avoided crossing is observed around the wavelength of the NK-2707 absorption, suggesting the system operates within the strong light-matter coupling regime. Using our TMR model we can describe the dispersion of the various polariton branches which we plot using open triangles. We can use the TMR model to determine the point at which the exciton and photon modes are degenerate in energy, and therefore identify the Rabi-splitting energy ($\hbar\Omega_{\text{rabi}}$) from the energetic separation between polariton states at this point. We then can equate the Rabi-splitting energy to the interaction potential (g) where $\hbar\Omega_{\text{rabi}} = 2g$. Using this approach, we find $2g = 120$ meV for the structure shown in Figure 2c. This interaction potential is larger than the half width at half maximum (HWHM) linewidth of the resonator optical modes ($\gamma_c = 80$ meV, corresponding to 25 nm) and the exciton of the J-aggregated dye ($\gamma_x = 25$ meV, corresponding

to 9 nm) and thus the structure meets the condition for strong coupling expressed using equation (1)⁴¹.

$$g^2 > (\gamma_c^2 + \gamma_x^2)/2 \quad (1)$$

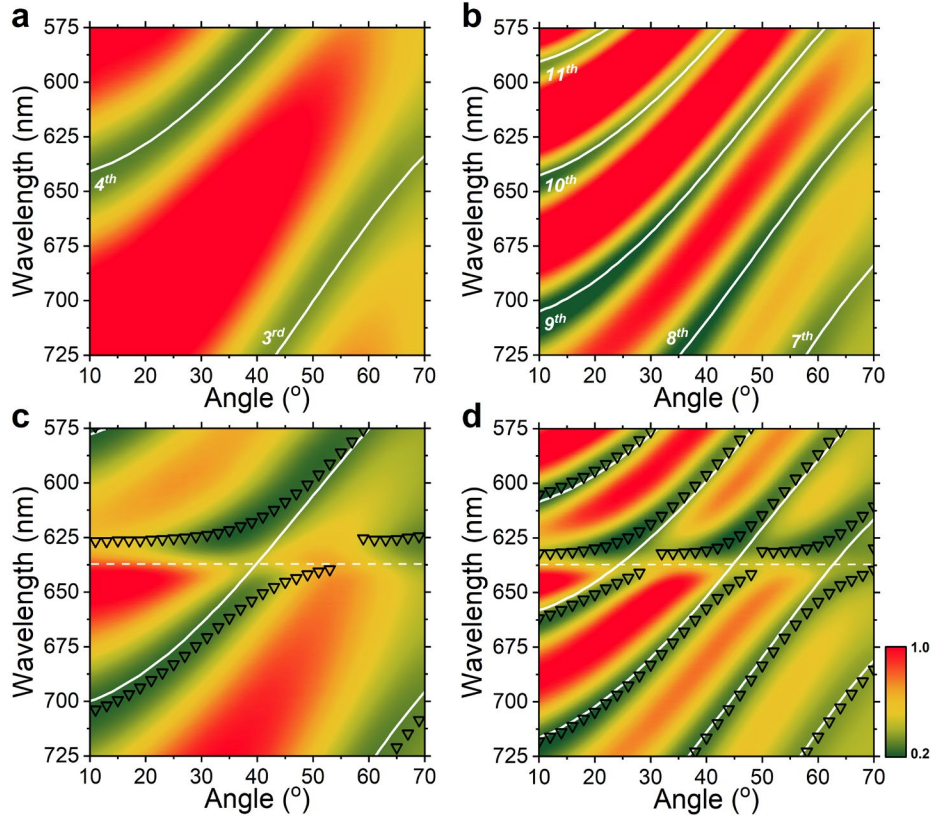


Figure 2. Angle-resolved reflectivity of dielectric slab microcavities. (a), (b) Angle-resolved white light reflectivity measurements of dielectric slab Fabry-Perot resonators without any top organic-semiconductor layer consisting of (a), 100 / 1000 nm and (b), 200 / 2300 nm Nb₂O₅ / SiO₂ layers respectively. (c), (d) Angular white light reflectivity spectra measured from the resonator structures of (a) and (b) when coated with NK-2707 / gelatine blend operating in the strong coupling regime. The white dashed lines show the exciton energy. TMR modelling is used to calculate the mode order, the dispersion of the uncoupled cavity modes (white solid lines) and the various polariton branches (open triangles).

In Figure 2d we plot the measured and modelled optical dispersion of the 8th, 9th and 10th optical modes as they undergo resonance with the NK-2707 dye at angles of 24°, 44° and

61° respectively. Again, we include a series of reflectivity spectra recorded at individual angles in Supporting Information Figure S2. Such optical properties are qualitatively similar to the ‘ladder’ of polariton states that we have observed in strong-coupled microcavities created using two silver-mirrors that contained a micron-thickness organic semiconductor film.⁴² Here, we use a TMR model to describe the dispersion of uncoupled photon modes (white solid lines) and the various polariton branches (open triangles). For the 8th order optical mode, our TMR model indicates a Rabi-splitting of 72 meV, however as the excitons couple to higher order modes (9th and 10th) the observed splitting reduces slightly as a result of a reduced overlap between the optical field and the organic layer. It is evident that the Rabi splitting energies observed in the structure whose optical properties are shown in Figure 2d are smaller than that evidenced in the thinner slab microcavity shown in Figure 2c. This effect results from the fact that the distribution of the electric field within the organic layer changes substantially as the cavity length of the structure is modified as can be seen in Figure 1b for the two different structures. It is also expected that structures composed of thicker dielectric layers have a higher Q-factor as a result of the longer round-trip propagation time.⁸ We find the HWHM linewidth of the uncoupled optical modes to reduce from $\gamma_c = 80$ meV in the thinner structure shown in Fig 2c, to $\gamma_c = 35$ meV for the thicker structure shown in Fig 2d. On the basis of the optical linewidths, we find that the condition for strong coupling expressed using equation 1 is also met for the structure shown in Fig 2d⁴¹.

For completeness, we have performed TMR simulations for a series of different Fabry-Perot resonators utilising metallic, dielectric or hybrid metallic-dielectric mirrors when filled with the same J-aggregate molecular dye that we compare to our dielectric slab resonator. The results of our simulations are tabulated in Table S1 of the Supporting Information where we compare the Q-factor and Rabi splitting energy of the different structures with experimental values determined from our dielectric-slab resonators. We also include in Figure S3 of the

Supporting Information experimental reflectivity spectra recorded from previous measurements on a selection of J-aggregate containing microcavities composed of (i) two silver mirrors, (ii) a silver and a dielectric mirror, (iii) two dielectric mirrors and (iv) a dielectric slab resonator. Here it can clearly be seen that strong coupling is evident in all types of structure studied.

Figure S4 and Figure S5 explore the effect of changing the thickness of the organic layer at the expense of the SiO₂ layer using TMR simulations. Here we assume that the number of molecules or their concentration is fixed or allowed to vary. This analysis confirms that Rabi-splitting increases as the square root as the number of molecules within the ‘cavity’. However, we predict an oscillatory behaviour in Rabi-splitting energy as the total number of molecules is held fixed but the thickness of the organic layer is varied. Here, we believe that this oscillatory effect results from (i) the change in the overlap of the organic excitons with the periodically varying electric field distribution and (ii) a shift of the energy of the confined optical modes due to changes in the effective refractive index of the cavity resulting from the changing organic layer thickness (i.e. different order modes become resonant with the excitons in the angular range probed by the simulations).

Figure S6 shows a simulation of the Rabi-splitting expected within a structure in which a thin, high oscillator-strength layer is placed at different locations within the organic film (e.g. at the SiO₂/organic interface, at the organic/air interface or at some intermediate position). This analysis indicates that the magnitude of the Rabi-splitting is dependent on the local electromagnetic field strength. Finally, Figure S7 shows a simulation of the dependence of the Rabi splitting energy as the thickness of the organic layer is held fixed, but the thickness of the SiO₂ layer is modified. Our analysis demonstrates that both Rabi-splitting and cavity mode linewidth increases as the SiO₂ thickness is reduced, with the structure operating in the strong-coupling regime for SiO₂ thicknesses greater than 100 nm.

Modifying optical properties through chemical reactions

The fact that the strongly coupled organic molecules are located close to the surface of the resonator opens the opportunity to determine whether we can use changes in optical properties of such structures to evidence optical changes driven by a simple chemical reaction. To do this, the surface of the slab resonator was coated with the porphyrin molecule meso-tetraphenyl-porphyrin (MTPP) dispersed in a polymeric matrix, with the chemical structure of MTPP shown in Figure 3a. This molecule was selected for experiment due to its relative narrow HWHM linewidth of $\gamma_x = 42$ meV (the first demonstration of strong coupling in an organic microcavity utilised a porphyrin²) together with the fact that porphyrins have been extensively used in sensing applications⁴³. Figure 3a (black solid line) plots the optical absorption of an unexposed 225 nm thick control film of a blend of MTPP dispersed in the polymer polystyrene (PS), with the MTPP / PS film created by spin-coating from a dichloromethane (DCM) solution. It can be seen that the film is characterised by a sharp absorption peak around 421 nm (peak labelled by a red dashed line) that we identify as the Soret band of MTPP and henceforth refer to as S1. We note that four additional weaker transitions are visible at longer wavelengths between 500 nm and 650 nm that correspond to the Q-bands of MTPP.

Figure 3a also shows the absorption spectra of the MTPP / PS control film following exposure to an HCl gas for a range of different times (data plotted using red solid lines). It can be seen that following 5 seconds of exposure, a second peak emerges at around 447 nm, labelled as S2 whose peak we identify using a blue dashed line. Notably, both excitonic states, S1 and S2, exhibit similar oscillator strengths. It can be seen that as the HCl exposure time is increased, the S1 peak becomes weaker; a process that is accompanied by an increase in oscillator strength of the S2 peak. This change in the optical properties of MTPP can be attributed to protonation of the porphyrin ring caused by exposure to the HCl gas⁴⁴. After around 600 seconds of HCl exposure, the S1 peak is reduced in intensity to the point that it only appears as a weak shoulder

at ~ 421 nm, with the S2 peak dominating the absorption. Note that the relative absorption strength of the various Q-bands also changes during the protonation of the porphyrin ring.

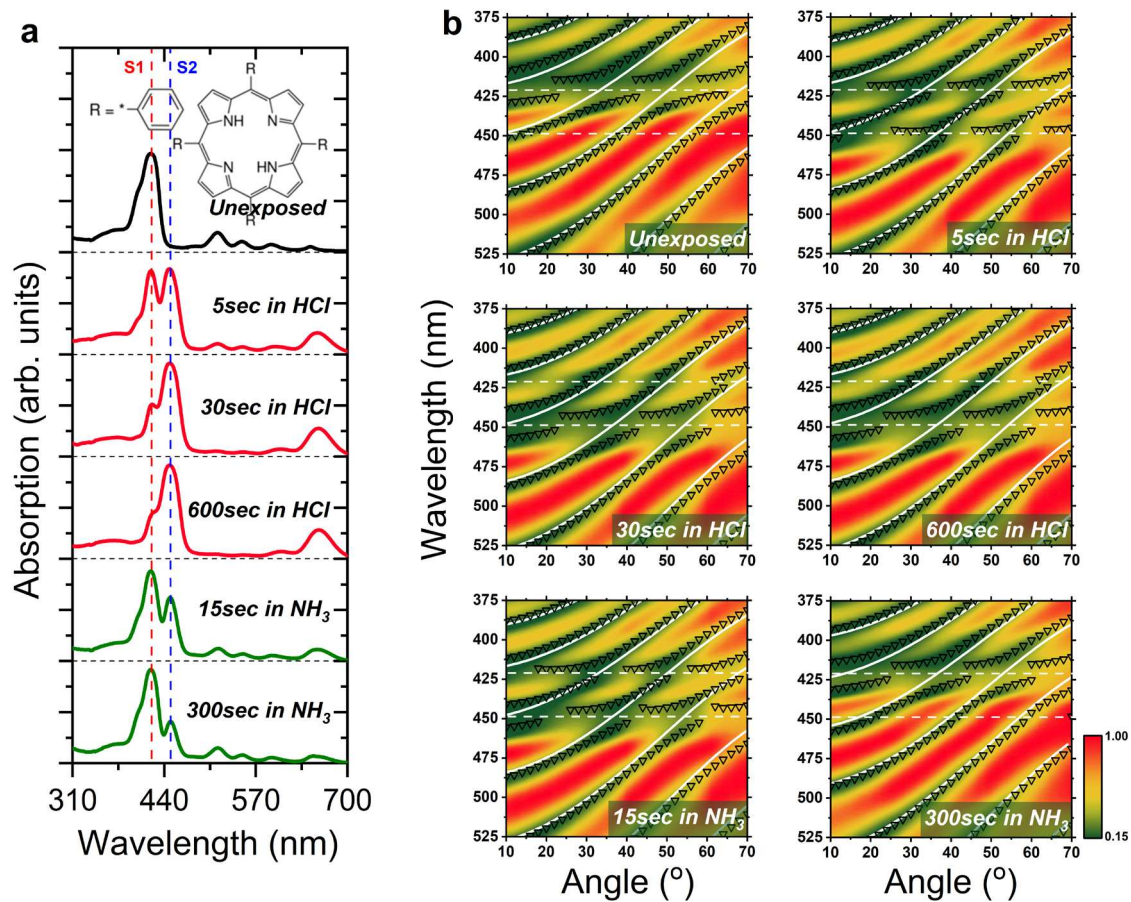


Figure 3. Reversible polariton ‘sensor’ using protonation and deprotonation of MTPP / PS blend. (a) Absorption spectrum of a 225 nm unexposed thin film of MTPP / PS blend (black solid line) along with its chemical structure. The absorption spectrum of the same film is also shown when exposed to an HCl gas for 5 seconds, 30 seconds and 600 seconds (red solid lines) and then exposed to an NH₃ gas for 15 seconds and 300 seconds (green solid lines). The peak wavelength of Soret band excitons S1 and S2 is indicated with red and blue dashed lines, respectively. (b) Angle-resolved white light reflectivity measurements from a slab resonator structure coated with a 225 nm MTPP / PS film when either unexposed, or when exposed to HCl for 5 seconds, 30 seconds and 600 seconds and to NH₃ for 15 seconds and 300 seconds. The dashed lines are a guide to the eye indicating the energy of the S1 and S2 excitons. A TMR model is used to describe the

dispersion of the uncoupled photon modes (solid lines) and dispersion of the various polariton branches (open triangles).

We can reverse the protonation of porphyrin by exposure to an NH_3 gas. This process is shown in Figures 3a (green solid lines), where it can be seen that deprotonation of the porphyrin ring leads to a suppression of the S2 peak accompanied by the re-emergence of the S1 peak at around 421 nm. It is worth noting that the deprotonation process is not completely reversible, and even after prolonged exposure to NH_3 gas (lasting several minutes), we do not fully recover the original absorption spectrum of the unexposed MTPP. This can be seen in Figure 3a where after 300 seconds of exposure to a NH_3 gas, there is still residual absorption at ~ 447 nm corresponding to the S2 peak. The origin of this effect is not currently understood, however it suggests that NH_3 molecules are not able to completely diffuse into the bulk of the film and fully deprotonate the MTPP.

We now turn our attention to a strongly coupled slab resonator whose surface is covered with a MTPP / PS film. Here, the structure explored consisted of 150 nm thick film of Nb_2O_5 coated with 1700 nm of SiO_2 and 225 nm of the MTPP / PS blend. This structure was again exposed to an HCl gas, followed by an NH_3 gas, with the angle-dependent white light optical reflectivity measured at various points during the gas exposure. Again, we include a series of reflectivity spectra recorded at individual angles in Supporting Information Figure S8. Figure 3b shows reflectivity data recorded at the same time points as those presented in Figure 3a for the control film. As it can be seen for the unexposed film in Figure 3b, we observe an anticrossing of reflectivity dips at a wavelength associated with the S1 porphyrin exciton, creating a lower (LPB) and upper (UPB) polariton branch. We include a TMR simulation of the dispersion of the various polaritonic modes as open triangles along with the photon mode dispersions (solid white lines) and S1 and S2 exciton energies (white dashed lines). Here, the Rabi-splitting energy between the LPB and UPB is 160 meV. Using HWHM linewidths for the

uncoupled optical resonator modes and the MTPP excitons as $\gamma_c = 66$ meV and $\gamma_x = 42$ meV, we confirm that this structure also operates in the strong-coupling regime.

This structure was then exposed to an HCl gas for 5 seconds. It can be seen that the reflectivity spectrum evolves into a distribution that can be described as a 3-way anticrossing corresponding to an optically driven hybridisation between the various photon modes and the S1 and S2 excitons. This is again described by a TMR model, with the emergence of a middle polariton branch (MPB) corresponding to a mixture between photon, S1 and S2 states identified in the figure, with the film expected to contain a mixture of protonated and unprotonated MTPP molecules. As the structure is further exposed to HCl, the S1 exciton state is relatively suppressed as the gas increasingly protonates the MTPP (30 sec HCl exposure). This results in the S1 exciton undergoing a transition from the strong to weak coupling regime; a process that leads to the apparent disappearance of the MPB as shown in Figure 3b following 600 seconds exposure to an HCl gas. At this point, an energetic anticrossing is only observed around a wavelength corresponding to the S2 exciton, with the LPB and UPB being clearly visible.

The structure was then exposed to an NH₃ gas for 15 seconds. After this exposure, both S1 and S2 excitons had sufficient oscillator strength to strongly couple to the photonic modes leading to the recovery of three hybridized polariton branches (LPB, MPB and UPB) as shown in Figure 3b. After 300 seconds of exposure, anticrossing is observed around 421 nm; a wavelength associated with the S1 transition of MTPP. This indicates that the chemical changes to the MTPP molecules are largely reversible.

We have used our TMR model to extract the interaction potential, g , between the S1 and S2 excitons and the confined photons as a function of time during exposure to the HCl gas as shown in Figure 4a. Note that in these experiments, the structure was exposed to a less concentrated gas environment to prolong the protonation process and increase experimental

resolution. Here, we define two regions of the plot that correspond to either weak or strong coupling regimes. We define these regions on the basis of the Rabi splitting energy ($\hbar\Omega_{\text{rabi}} = 2g$) and the HWHM linewidth of the exciton and the photon mode as expressed by equation (1)⁴¹. It can be seen that during the HCl gas exposure, we observe a correlated increase and reduction in the interaction potential for S2 and S1 transitions respectively.

At present we have not yet undertaken a controlled study of the rate at which protonation / deprotonation rates occurs in our structures, and we are presently unable to determine whether such structures can be used to modify chemical reactions. Nevertheless, we believe that the ability to follow a simple chemical reaction involving strongly coupled molecules positioned close to a surface makes this an interesting structure for more detailed studies.

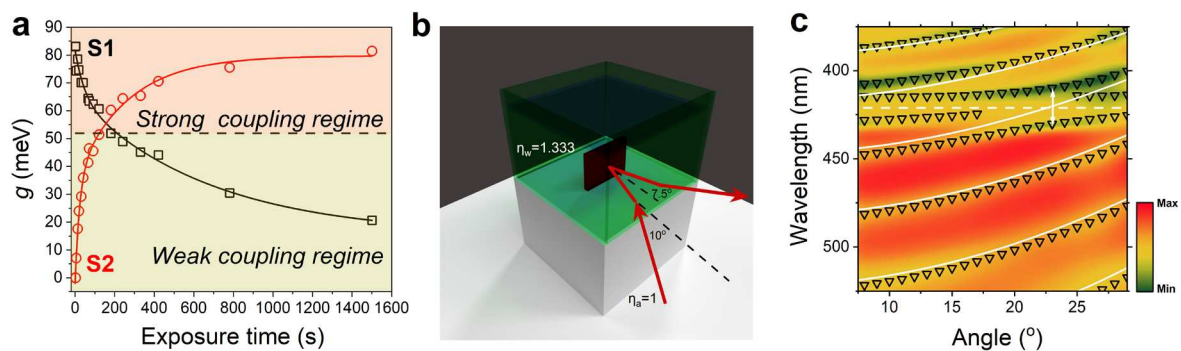


Figure 4. Interaction potential of excitons S1 and S2 with HCl gas exposure and strong coupling in water. (a) Interaction potential g between confined photonic modes and excitons S1 and S2 as a function of exposure time to an HCl gas, with the strong and weak coupling regimes for each state defined⁴¹. Black and red solid lines are a guide to the eye. (b) Schematic of the resonator immersed in water with a measurement of white light reflectivity. Here, the angle of incidence in air is 10° while in water it is 7.5° assuming the refractive index of 1.333. (c) Angle-resolved white reflectivity measurement of a resonator coated with MTPP / PS when fully immersed in water. The goniometer arms were tuned between 10° to 40° in air; an angular range that corresponds to

angles between 7.5° and 29° in an aqueous environment. Using a TMR model we mark the exciton energy with a white dashed line, the uncoupled optical modes with white solid lines and the various polaritons modes with open triangles. White arrows indicate the avoided crossing between two polariton branches around 23°.

Strong coupling in water

We have measured angular white light reflectivity of a typical resonator structure immersed in water. Here, Figure 4b shows a schematic of the experimental setup where we account for the difference in refractive index between air and water. In this experiment, the dielectric slab was coated with a MTPP / PS film with white light optical reflectivity confirming a mode splitting around the S1 exciton wavelength as shown in Figure 4c at an angle around 23°. Using a TMR model to describe the dispersion of the various modes, we determine a Rabi-splitting energy ($2g$) of 145 meV. Here, our model indicates that the reflectivity of the interface between the organic layer and water is reduced to around 2%. Using measured HWHM linewidths of the uncoupled resonator modes and the exciton to be $\gamma_c = 72$ meV and $\gamma_x = 42$ meV, we again determine that this structure operates in the strong coupling regime. For clarity, we re-plot data of Figure 4c in Figure S9 of the Supporting Information around the wavelength region 400 - 450 nm and also show a cross-section of the reflectivity map measured around resonance. This experiment demonstrates the ability of a strong-coupled slab resonator to operate in the strong coupling regime when fully immersed in solution.

Simulated vibrational strong-coupling

Finally, we have performed optical modelling to explore whether similar structures to those described above could be used to generate vibrational strong coupling^{45,46}. Here we used a TMR model to describe a structure in which a 2000 nm thick layer characterised by an

optically allowed transition having an oscillator strength that is typical of the C = O vibronic modes in the polymer PMMA is combined with two different dielectric materials that are otherwise optically inert in the IR region (namely CaF₂ and ZnSe). Here, these materials are widely used in IR spectroscopy, with their low and high refractive index resulting in optical confinement within a slab-based structure. Our simulations (see Figure S10 and Table S2 of the Supporting Information) confirm that such microcavities can support vibrational strong coupling in a regime where the majority of the polaritonic chemistry experiments reported have been performed^{10,14,16,47}. This finding suggests that our structures may well be applicable as a platform to facilitate polaritonic chemistry. We note that previous experiments in which vibrational strong coupling has been used to change chemical reaction rates have been performed in solution-based studies in which the reaction solution of interest is introduced between two closely spaced mirrors. Here, our geometry would require the reacting species to be either dispersed within a polymeric film, covalently attached to a polymer backbone or otherwise bound or adsorbed to a surface. We expect this geometry to be favourable for reaction-rate studies, as it should be possible to carefully control whether the reacting species is in the weak or strong-coupling regime by adjusting the thickness of the CaF₂ dielectric layer (see Figure S7), making well-controlled experiments relatively easier to perform.

CONCLUSIONS

We have developed a new photonic structure based on a low index dielectric slab that is coated with an organic semiconducting film with the organic dye molecules being strongly coupled to a confined optical mode that extends into the surface layer. A porphyrin-doped polymer layer was coated onto the surface of the dielectric slab and the protonation and deprotonation of the porphyrin ring was followed through the strong coupling of two excitonic states that can be driven into the weak or strong coupling regime by exposure of the surface to a HCl or NH₃ gas. At present, our measurements do not indicate whether our structure is able

to enhance or suppress this chemical process. However we note that our structures should act as a platform to study chemical processes in which molecular materials are both strong-coupled and are completely open to a gaseous or liquid environment. Indeed, by modelling a structure that includes optical-constants typical of a C = O vibrational mode, our TMR simulations confirm that such structures can potentially be used for vibrational strong coupling in the IR region.

ASSOCIATED CONTENT

Supporting Information

The supporting information is available free of charge at

Experimental methods. Cross section of reflectivity maps in empty microcavities. Cross section of reflectivity maps in NK-2707 microcavities. Simulated strong-coupling in different Fabry-Perot resonator types. TMR modelling for different SiO₂ / organic layer thicknesses. Cross section of reflectivity maps in MTPP microcavities. Strong coupling in water. Simulated vibrational strong coupling.

AUTHOR INFORMATION

Corresponding Authors

Kyriacos Georgiou – Department of Physics and Astronomy, University of Sheffield, Hicks Building, Hounsfield Road, Sheffield S3 7RH, United Kingdom; Department of Physics, University of Cyprus, P. O. Box 20537, Nicosia 1678, Cyprus;

orcid.org/0000-0001-5744-7127

email: k.georgiou@sheffield.ac.uk

David G. Lidzey – Department of Physics and Astronomy, University of Sheffield, Hicks Building, Hounsfield Road, Sheffield S3 7RH, United Kingdom;

orcid.org/0000-0002-8558-1160

email: d.g.lidzey@sheffield.ac.uk

Author

Rahul Jayaprakash – Department of Physics and Astronomy, University of Sheffield, Hicks Building, Hounsfield Road, Sheffield S3 7RH, United Kingdom;

orcid.org/0000-0002-2021-1601

email: r.jayaprakash@sheffield.ac.uk

Authors Contributions

K.G. fabricated the samples and then designed and performed the optical experiments. K.G. analysed the data. R.J. performed the transfer matrix reflectivity modelling. K.G. wrote the manuscript with significant contributions from D.G.L. K.G. and D.G.L. conceived the idea. D.G.L. supervised the project.

Notes

D.G.L. is the chairman of the company Ossila Ltd that retails organic semiconductor materials and thin-film process and test equipment.

ACKNOWLEDGEMENTS

We thank the U.K. EPSRC for funding this research via the Programme Grant ‘Hybrid Polaritonics’ (EP/M025330/1).

REFERENCES

- (1) Weisbuch, C.; Nishioka, M.; Ishikawa, A.; Arakawa, Y. Observation of the Coupled Exciton-Photon Mode Splitting in a Semiconductor Quantum Microcavity. *Phys. Rev.*

- Lett.* **1992**, *69* (23), 3314–3317.
- (2) D. G. Lidzey; Bradley, D. D. C.; Skolnick, M. S.; Virgili, T.; Walker, S.; Whittaker, D. M. Strong Exciton-Photon Coupling in an Organic Semiconductor Microcavity. *Lett. to Nat.* **1998**, *395*, 53–55.
 - (3) Plumhof, J. D.; Stoeflerle, T.; Mai, L.; Scherf, U.; Mahrt, R. F. Room-Temperature Bose-Einstein Condensation of Cavity Exciton-Polariton in a Polymer. *Nat. Mater.* **2014**, *13*, 247–252.
 - (4) Daskalakis, K. S.; Maier, S. A.; Murray, R.; Kéna-cohen, S. Nonlinear Interactions in an Organic Polariton Condensate. *Nat. Mater.* **2014**, *13*, 271–278.
 - (5) Cookson, T.; Georgiou, K.; Zasedatelev, A.; Grant, R. T.; Virgili, T.; Cavazzini, M.; Galeotti, F.; Clark, C.; Berloff, N. G.; Lidzey, D. G.; et al. A Yellow Polariton Condensate in a Dye Filled Microcavity. *Adv. Opt. Mater.* **2017**, *5* (18), 1700203.
 - (6) Sanvitto, D.; Kéna-Cohen, S. The Road towards Polaritonic Devices. *Nat. Mater.* **2016**, *15*, 1061–1073.
 - (7) Zasedatelev, A. V.; Baranikov, A. V.; Urbonas, D.; Scafirimuto, F.; Scherf, U.; Stöferle, T.; Mahrt, R. F.; Lagoudakis, P. G. A Room-Temperature Organic Polariton Transistor. *Nat. Photonics* **2019**, *13*, 378–383.
 - (8) Kavokin, A. V.; Baumberg, J. J.; Malpuech, G.; Laussy, F. P. *Microcavities*, Second Edi.; Oxford Univ. Press, 2007.
 - (9) Hutchison, J. A.; Liscio, A.; Schwartz, T.; Canaguier-Durand, A.; Genet, C.; Palermo, V.; Samorì, P.; Ebbesen, T. W. Tuning the Work-Function via Strong Coupling. *Adv. Mater.* **2013**, *25*, 2481–2485.
 - (10) Thomas, A.; Lethuillier-Karl, L.; Nagarajan, K.; Vergauwe, R. M. A.; George, J.;

- Chervy, T.; Shalabney, A.; Devaux, E.; Genet, C.; Moran, J.; et al. Tilting a Ground-State Reactivity Landscape by Vibrational Strong Coupling. *Science* (80-.). **2019**, *363* (6427), 615–619.
- (11) Hertzog, M.; Wang, M.; Mony, J.; Börjesson, K. Strong Light-Matter Interactions: A New Direction within Chemistry. *Chem. Soc. Rev.* **2019**, *48*, 937–961.
- (12) Coles, D. M.; Somaschi, N.; Michetti, P.; Clark, C.; Lagoudakis, P. G.; Savvidis, P. G.; Lidzey, D. G. Polariton-Mediated Energy Transfer between Organic Dyes in a Strongly Coupled Optical Microcavity. *Nat. Mater.* **2014**, *13*, 712–719.
- (13) Georgiou, K.; Michetti, P.; Gai, L.; Cavazzini, M.; Shen, Z.; Lidzey, D. G. Control over Energy Transfer between Fluorescent BODIPY Dyes in a Strongly-Coupled Microcavity. *ACS Photonics* **2018**, *5* (1), 258–266.
- (14) Vergauwe, R. M. A.; Thomas, A.; Nagarajan, K.; Shalabney, A.; George, J.; Chervy, T.; Seidel, M.; Devaux, E.; Torbeev, V.; Ebbesen, T. W. Modification of Enzyme Activity by Vibrational Strong Coupling of Water. *Angew. Chemie - Int. Ed.* **2019**, *58* (43), 15324–15328.
- (15) Stranius, K.; Hertzog, M.; Börjesson, K. Selective Manipulation of Electronically Excited States through Strong Light-Matter Interactions. *Nat. Commun.* **2018**, *9*, 2273.
- (16) Thomas, A.; George, J.; Shalabney, A.; Dryzhakov, M.; Varma, S. J.; Moran, J.; Chervy, T.; Zhong, X.; Devaux, E.; Genet, C.; et al. Ground-State Chemical Reactivity under Vibrational Coupling to the Vacuum Electromagnetic Field. *Angew. Chemie - Int. Ed.* **2016**, *55* (38), 11462–11466.
- (17) Herrera, F.; Spano, F. C. Cavity-Controlled Chemistry in Molecular Ensembles. *Phys. Rev. Lett.* **2016**, *116* (23), 238301.

- (18) Ribeiro, R. F.; Martínez-Martínez, L. A.; Du, M.; Campos-Gonzalez-Angulo, J.; Yuen-Zhou, J. Polariton Chemistry: Controlling Molecular Dynamics with Optical Cavities. *Chem. Sci.* **2018**, *9* (30), 6325–6339.
- (19) Feist, J.; Galego, J.; García-Vidal, F. J. Polaritonic Chemistry with Organic Molecules. *ACS Photonics* **2018**, *5* (1), 205–216.
- (20) Herrera, F.; Owrutsky, J. Molecular Polaritons for Controlling Chemistry with Quantum Optics. *J. Chem. Phys.* **2020**, *152* (10), 100902.
- (21) Campos-Gonzalez-Angulo, J. A.; Ribeiro, R. F.; Yuen-Zhou, J. Resonant Catalysis of Thermally Activated Chemical Reactions with Vibrational Polaritons. *Nat. Commun.* **2019**, *10* (1), 1–8.
- (22) Schwartz, T.; Hutchison, J. A.; Genet, C.; Ebbesen, T. W. Reversible Switching of Ultrastrong Light-Molecule Coupling. *Phys. Rev. Lett.* **2011**, *106* (19), 196405.
- (23) Hutchison, J. A.; Schwartz, T.; Genet, C.; Devaux, E.; Ebbesen, T. W. Modifying Chemical Landscapes by Coupling to Vacuum Fields. *Angew. Chemie - Int. Ed.* **2012**, *51*, 1592–1596.
- (24) Connolly, L. G.; Lidzey, D. G.; Butté, R.; Adawi, A. M.; Whittaker, D. M.; Skolnick, M. S. Strong Coupling in High-Finesse Organic Semiconductor Microcavities. *Appl. Phys. Lett.* **2003**, *83* (26), 5377–5379.
- (25) Coles, D. M.; Flatten, L. C.; Sydney, T.; Hounslow, E.; Saikin, S. K.; Aspuru-Guzik, A.; Vedral, V.; Tang, J. K. H.; Taylor, R. A.; Smith, J. M.; et al. A Nanophotonic Structure Containing Living Photosynthetic Bacteria. *Small* **2017**, *13*, 1701777.
- (26) Flatten, L. C.; Christodoulou, S.; Patel, R. K.; Buccheri, A.; Coles, D. M.; Reid, B. P. L.; Taylor, R. A.; Moreels, I.; Smith, J. M. Strong Exciton-Photon Coupling with

- Colloidal Nanoplatelets in an Open Microcavity. *Nano Lett.* **2016**, *16*, 7137–7141.
- (27) Barnes, W. L.; Preist, T.; Kitson, S.; Sambles, J. Physical Origin of Photonic Energy Gaps in the Propagation of Surface Plasmons on Gratings. *Phys. Rev. B - Condens. Matter Mater. Phys.* **1996**, *54* (9), 6227–6244.
- (28) Wan, W.; Yang, X.; Gao, J. Strong Coupling between Mid-Infrared Localized Plasmons and Phonons. *Opt. Express* **2016**, *24* (11), 12367.
- (29) Yao, Y.-F.; Lin, C.-H.; Chao, C.-Y.; Chang, W.-Y.; Su, C.-Y.; Tu, C.-G.; Kiang, Y.-W.; Yang, C. C. Coupling of a Light-Emitting Diode with Surface Plasmon Polariton or Localized Surface Plasmon Induced on Surface Silver Gratings of Different Geometries. *Opt. Express* **2018**, *26* (7), 9205.
- (30) Berrier, A.; Cools, R.; Arnold, C.; Offermans, P.; Crego-Calama, M.; Brongersma, S. H.; Gómez-Rivas, J. Active Control of the Strong Coupling Regime between Porphyrin Excitons and Surface Plasmon Polaritons. *ACS Nano* **2011**, *5* (8), 6226–6232.
- (31) Castellanos, G. W.; Murai, S.; Raziman, T. V.; Wang, S.; Ramezani, M.; Curto, A. G.; Gómez Rivas, J. Exciton-Polaritons with Magnetic and Electric Character in All-Dielectric Metasurfaces. *ACS Photonics* **2020**, *7* (5), 1226–1234.
- (32) Todisco, F.; Malureanu, R.; Wolff, C.; Gonçalves, P. A. D.; Roberts, A. S.; Asger Mortensen, N.; Tserkezis, C. Magnetic and Electric Mie-Exciton Polaritons in Silicon Nanodisks. *Nanophotonics* **2020**, *9* (4), 803–814.
- (33) Giebink, N. C.; Wiederrecht, G. P.; Wasielewski, M. R. Strong Exciton-Photon Coupling with Colloidal Quantum Dots in a High- Q Bilayer Microcavity. *Appl. Phys. Lett.* **2011**, *98* (8), 1–4.

- (34) Lerario, G.; Ballarini, D.; Fieramosca, A.; Cannavale, A.; Genco, A.; Mangione, F.; Gambino, S.; Dominici, L.; De Giorgi, M.; Gigli, G.; et al. High-Speed Flow of Interacting Organic Polaritons. *Light Sci. Appl.* **2017**, *6*, e16212.
- (35) Hecht, E. *Optics*, Fourth Edi.; 2002.
- (36) Jelley, E. E. Spectral Absorption and Fluorescence of Dyes in the Molecular State. *Nature* **1936**, *138*, 1009–1010.
- (37) Lidzey, D. G.; Fox, a. M.; Rahn, M.; Skolnick, M. S.; Agranovich, V. M.; Walker, S. Experimental Study of Light Emission from Strongly Coupled Organic Semiconductor Microcavities Following Nonresonant Laser Excitation. *Phys. Rev. B* **2002**, *65* (19), 195312.
- (38) Coles, D. M.; Michetti, P.; Clark, C.; Tsoi, W. C.; Adawi, A. M.; Kim, J. S.; Lidzey, D. G. Vibrationally Assisted Polariton-Relaxation Processes in Strongly Coupled Organic-Semiconductor Microcavities. *Adv. Funct. Mater.* **2011**, *21* (19), 3691–3696.
- (39) Coles, D. M.; Grant, R. T.; Lidzey, D. G.; Clark, C.; Lagoudakis, P. G. Imaging the Polariton Relaxation Bottleneck in Strongly Coupled Organic Semiconductor Microcavities. *Phys. Rev. B* **2013**, *88* (12), 121303.
- (40) Paschos, G. G.; Somaschi, N.; Tsintzos, S. I.; Coles, D. M.; Bricks, J. L.; Hatzopoulos, Z.; Lidzey, D. G.; Lagoudakis, P. G.; Savvidis, P. G. Hybrid Organic-Inorganic Polariton Laser. *Sci. Rep.* **2017**, *7*, 11377.
- (41) Savona, V.; Andreani, L. C.; Schwendimann, P.; Quattropani, A. Quantum Well Excitons in Semiconductor Microcavities: Unified Treatment of Weak and Strong Coupling Regimes. *Solid State Commun.* **1995**, *93* (9), 733–739.
- (42) Coles, D. M.; Lidzey, D. G. A Ladder of Polariton Branches Formed by Coupling an

- Organic Semiconductor Exciton to a Series of Closely Spaced Cavity-Photon Modes. *Appl. Phys. Lett.* **2014**, *104* (19), 191108.
- (43) Paolesse, R.; Nardis, S.; Monti, D.; Stefanelli, M.; Di Natale, C. Porphyrinoids for Chemical Sensor Applications. *Chem. Rev.* **2017**, *117* (4), 2517–2583.
- (44) Muthukumar, P.; John, S. A. Highly Sensitive Detection of HCl Gas Using a Thin Film of Meso-Tetra(4-Pyridyl)Porphyrin Coated Glass Slide by Optochemical Method. *Sensors and Actuators, B: Chemical*. 2011, pp 238–244.
- (45) Long, J. P.; Simpkins, B. S. Coherent Coupling between a Molecular Vibration and Fabry-Perot Optical Cavity to Give Hybridized States in the Strong Coupling Limit. *ACS Photonics* **2015**, *2* (1), 130–136.
- (46) Shalabney, A.; George, J.; Hutchison, J.; Pupillo, G.; Genet, C.; Ebbesen, T. W. Coherent Coupling of Molecular Resonators with a Microcavity Mode. *Nat. Commun.* **2015**, *6*, 5981.
- (47) Dunkelberger, A. D.; Spann, B. T.; Fears, K. P.; Simpkins, B. S.; Owrutsky, J. C. Modified Relaxation Dynamics and Coherent Energy Exchange in Coupled Vibration-Cavity Polaritons. *Nat. Commun.* **2016**, *7*, 1–10.